Title

GAMMA-RAY IMAGING USING A FRESNEL ZONE PLATE APERTURE, MULTIWIRE PROPORTIONAL CHAMBER DETECTOR, AND COMPUTER RECONSTRUCTION

Authors

Macdonald, B.
Chang, L.T.
Perez-Mendez, V.
et al.

Publication Date

1973-11-01

Presented at the IEEE Nuclear Science
Symposium, San Francisco, California,
November 14-16, 1973.

LBL-2048
c.1

GAMMA-RAY IMAGING USING A FRESNEL ZONE PLATE APERTURE, MULTIWIRE PROPORTIONAL CHAMBER DETECTOR, AND COMPUTER RECONSTRUCTION

B. Macdonald, L. T. Chang, V. Perez-Mendez and L. Shiraishi

November 1973

Prepared for the U. S. Atomic Energy Commission
under Contract W-7405-ENG-48

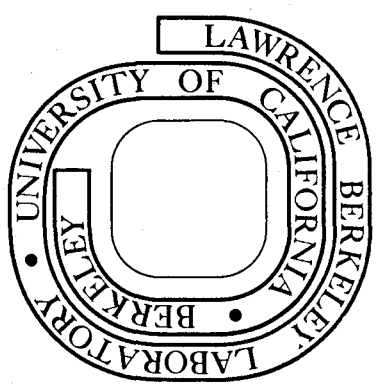

LBL-2048
c.1

DISCLAIMER

GAMMA-RAY IMAGING USING A FRESNEL ZONE PLATE APERTURE, MULTIWIRE PROPORTIONAL CHAMBER DETECTOR, AND COMPUTER RECONSTRUCTION

B. Macdonald, L. T. Chang, V. Perez-Mendez, and L. Shiraishi

Lawrence Berkeley Laboratory
University of California
Berkeley, California

Abstract

The use of the multiwire proportional chamber in a Fresnel zone plate coded aperture gamma-ray imaging system is described. Image reconstruction is by computer using the fast Fourier transform algorithm. Criteria for design parameters of the imaging system are established. A calculation of the signal/noise ratio of images reconstructed from computer-generated on-axis zone plate holograms gives values, for larger numbers of gamma-ray events, which are somewhat smaller than theoretical values based on a shot-noise formula. The use of a positive and a negative zone plate combination is shown to eliminate the large background usually associated with on-axis zone plate imaging.

Introduction

There has recently been considerable interest in the use of the Fresnel zone plate coded aperture for imaging sources having continuous distributions of gamma-ray emission, especially for nuclear medicine applications.[1] Motivation for this interest has come from the greatly increased gamma-ray collection efficiency (several orders of magnitude) of these apertures compared with a pinhole collimator of the same resolution and second, from the ability of the system to provide three dimensional images. In coded aperture imaging the source distribution casts a shadow of the aperture on the detector (Fig. 1). This shadow hologram has, to the eye, little relationship to the original object and must be decoded to obtain the image. Decoding can be done coherently using a laser for example, or incoherently using a similar zone plate as a mask. We describe later the use of the computer for decoding.

The imaging process can be understood by considering the object to be the sum of a number of point sources. A given point in the object casts a gamma-ray shadow of the zone plate on the detector. This shadow is itself a zone plate and, in reconstructing the original object point, use is made of the property of a zone plate to focus light to a point by diffraction, the transverse position depending on the center of the zone plate shadow system. Information about the depth comes from the size of the zone plate shadow on the hologram, the larger shadows being cast by object points closer to the zone plate.

The zone plate aperture consists of concentric circles of radii $R_n = \sqrt{n}\,R_1$. The area between adjacent circles is either opaque or transparent to the detected radiation, the opaque and transparent zones alternating. If the first zone is transparent the aperture is called a positive zone plate; if opaque, negative. Zone plates for 100 keV gammas with 50 or more zones are easily made from 1.5 mm thick lead.

Our detector is the multiwire proportional chamber with delay-line readout which has the ability to record a shadow hologram either photographically from an oscilloscope screen or in digitized form on magnetic tape. Since we had digitized data available we have investigated computer reconstruction since there are advantages of this method compared with using film. The hologram has a large dynamic range which constitutes a problem for film. Image noise contributed by film grain can be considerable.[2] Results with the computer can be obtained quickly without the delay associated with a two-step photographic process. There are obvious advantages in image processing with the computer. There are, of course, disadvantages since optical reconstruction involves simple, inexpensive equipment.

Zone Plate Imaging System Parameters

The zone plate imaging system is characterized by the following independent parameters (Fig. 1):

- S_1 Object plane to zone plate distance,
- S_2 Zone plate to detector distance,
- U Detector size,
- D Diameter of the zone plate,
- N_d Number of detector resolution lengths, (detector size/detector resolution length),
- N_z Number of zones in the zone plate.

It is convenient to consider objects restricted to be only within the object plane field of view V. It is possible to get images from objects located outside the field of view but they are detected with less efficiency than if they were within V and the image of a point source is no longer a circle. We also restrict ourselves to objects which lie in a lateral plane. Although one of the principal features of the zone plate imaging system is that it has depth resolution, we do not consider this here.

The resolution of the image is determined by the width of the finest zone, $W = D/4N_z$. This resolution, when referred back to the object plane, is $\delta x = (1 + S_1/S_2)D/4N_z$. Let N be the number of resolution lengths in the object field of view, $N = V/\delta x$. Define S, the field of view parameter, as

$$S = \frac{V/D}{(1 + S_1/S_2)}$$

$$\text{then } N = 4N_z S \ .$$

When the object plane is at point A, S = 0 and the number, N, of resolution lengths in the object field of view is zero. The resolution, δx, has its smallest value there.

$$\delta x_{min} = \frac{U}{4 N_z (U/D - 1)}$$

If the detector can resolve $W = D/4N_z$ directly, then the limiting object plane B in Fig. 1 is at $S_1 = \infty$. If it cannot then B is located where the detector can just resolve the shadow of the finest zone and N, S, and δx have their maximum values there.

$$N_{max} = N_d - 4 N_z$$

$$S_{max} = N_d/4 N_z - 1$$

$$\delta x_{max} = \frac{U}{4 N_z U/D - N_d}$$

We see that good resolution is obtained when N_z is large and when $U \gg D$. Values of S_{max}, N_{max}, and N_z are listed in Table I for various values of N_d. Thus, with a given detector of size U and number of resolution lengths, N_d, and given the largest object, N_{max}, to be imaged, N_z and S_{max} are determined. The zone plate diameter D then gives the range of resolutions δx obtainable. Solid angle considerations determine S_1 or S_2.

Image Reconstruction by Computer

Optical image reconstruction of a zone plate shadow hologram uses the property of the Fresnel zone plate that it acts like a lens, light passing through it being diffracted and coming to a focus. A converging lens is often used after the zone plate shadow hologram to bring the point of focus closer to the hologram. In computer reconstruction we take advantage of the fact that the light intensity in the back focal plane of a lens is proportional to the square modulus of the Fourier transform of the light amplitude incident on the lens.

A diagram of the optical analogue of our computer image reconstruction scheme is given in Fig. 2. In the hologram plane is the zone plate shadow of a single point source. This zone plate shadow has a focal length f for light of wavelength λ, $f = D'^2/4N_z\lambda$. All zone plate shadows of point objects in a given object plane have the same diameter D' and therefore a given value of f represents one object plane. Because of the focussing properties of the zone plate, light from the point O, a distance f away from the zone plate shadow, comes out in a parallel beam. This parallel light is focussed to a point in the back focal plane of the lens. The position of this point in the back focal plane depends on the center of the zone plate shadow and therefore on the position of that source point which produced this shadow. Choosing the light source at O ensures that the image plane and the back focal plane of the Fourier transform lens coincide. Thus, with this geometry, we can get an image of the original object plane by taking a Fourier transform of the light amplitude in the hologram plane.

A hologram matrix is formed in the computer by binning the (x,y) coordinates of gamma-ray events measured by the detector into a matrix of dimensions $N_h \times N_h$. Since this matrix must be able to resolve the shadow of the finest zone, N_h is usually somewhat greater than N_d. We then take the square root of these binned elements to obtain the amplitude transmission matrix, and multiply by a complex quadratic phase factor, Φ, which represents light diverging from a point a distance f away.

$$\Phi = e^{i \frac{\pi r^2}{\lambda f}},$$

where r is the distance from the center of the hologram. The resulting complex matrix is then Fourier transformed using the fast Fourier transform algorithm (FFT).[3] The image matrix is obtained by taking the square modulus of the resulting complex matrix elements. Note that there is no dependence on the wavelength of light since Φ depends on λf which is just $D'^2/4 N_z$, independent of λ.

Using our optical analogue and the definition of the fast Fourier transform we get the following expression for the number ΔK of image rasters for the width of the field of view in the image matrix.

$$\Delta K = 4 N_z S (1 + S)$$

where, as before, N_z is the number of zones in the zone plate and S is the field of view parameter. That ΔK does not depend on the dimension of the image matrix is at first surprising but comes from the fact that the unit of frequency in the matrix resulting from using the FFT algorithm is just 1/U, U being the detector width. Since $4 N_z S$ is the number of resolution lengths in the field of view we can see that the number of image rasters in one resolution length is just 1 + S.

At present our computer reconstruction programs use the CDC 7600 computer at the Lawrence Berkeley Laboratory which has a cycle time of 0.03 μsec and can hold a complex 512 × 512 matrix. About 12 seconds of central processor time is required to bin a million events in the hologram matrix. The FFT algorithm takes about 4 seconds to make a transform of a complex 256 × 256 matrix, the time for larger arrays scaling as $N_h^2 \log_2 N_h^2$. In collaboration with Dr. Thomas Budinger of the Donner Laboratory we are developing zone plate imaging programs which will fit into a small computer having magnetic disc storage. For the Hewlett Packard 5407A computer the time for FFT for a 64 x 64 matrix is 30 seconds.

Computer reconstruction of a hologram of random gamma-ray events that was generated by computer is given in Fig. 3. The object was a 256 point square array of point sources of equal intensities with the point separation chosen to be 2-1/2 resolution lengths. Background for point-like objects can be eliminated by frequency filtering and this has been done in Fig. 4. Plots of cross-sections through these images, Fig. 5, show clearly the large background associated with imaging using the on-axis zone plate. This background has dictated the choice here of a point-like object. We show later how this background can be eliminated even for a continuous source distribution with low spatial frequencies.

Signal/Noise Ratio

We can also see from Fig. 5 the characteristic noise due to the random nature of the gamma-ray events. This noise, causing a statistical variation of the peak heights, is a severe limitation of the zone plate imaging system. Barrett has made an approximate calculation of the signal/noise ratio using an analogy with shot-noise.[4]

$$(S/N)_B = \frac{2}{\pi} \sqrt{\frac{C}{M^2}},$$

where C is the number of events in the hologram and M is the number of object points or of resolution areas in the object.

In comparison, the pinhole camera has a signal/noise ratio given by $(S/N)_{PH} = \sqrt{C_{PH}/M}$. Thus, the noise for zone plate imaging increases much faster with M than it does for a pinhole camera and the geometrical advantage of the zone plate is sharply reduced for objects having larger numbers of resolution areas.

Because of the importance of the signal/noise ratio for zone plate imaging we have measured this quantity for gamma-ray events generated by the computer. We distribute M point sources of equal intensity in a square array uniformly over the field of view. A number of gamma-ray events, corresponding to a given value of $(S/N)_B$, were randomly generated, the image obtained by the fast Fourier transform, and the image point peak intensities, which included background, were obtained. The average background for the image of a given object point was found by taking the average of four values in the neighborhood of that point at a distance such that the signal from the point was small. This distance was 2 raster points in all cases. Subtracting this average background for a given peak from the intensity of the peak gave the signal intensity for that object point.

The noise was taken to be the standard deviation of the set of M signals. However, in order to get a statistical accuracy of about 10%, when M was less than 100 the process was repeated with statistically independent holograms and the set of signals augmented until it numbered about 100. The signal/noise ratio is then the average of the signals divided by their standard deviation. Because our method for subtracting the background causes the noise to be slightly overestimated the S/N ratio in our measurements should be multiplied by the factor $\sqrt{5/4}$. This correction has been incorporated in Table II which compares our corrected measured values with the theoretical value $(S/N)_B$ for various numbers of object points. Errors quoted are statistical errors only. The table spans a range of gamma-ray events from 800 to 16 million.

Background Elimination with the On-Axis Zone Plate

We have already shown one method for reducing the image background associated with the on-axis Fresnel zone plate imaging system--frequency filtering of a point-like object. If the object is not point-like it can be made so by placing over the object a half-tone screen of crossed grids with a resulting attenuation of count-rate of about a factor of 4.

Another method that has been used to reduce image background is the off-axis zone plate, a circular section of the on-axis zone plate that does not include the center. This method also requires the use of the half-tone screen. A further disadvantage is that in order to obtain an image of the same resolution the detector must have 2 to 3 times better resolution than in the on-axis case. This is acceptable if the detector is photographic film but is undesirable for detectors such as the multiwire proportional chamber or the image intensifier tube with their 1 mm resolutions.

A new method for background elimination that does not involve either the half-tone screen or the off-axis zone plate is the use of a combination of positive and negative zone plates. The basis for the method can be seen from an examination of the equations that govern image formation with the zone plate system. The hologram amplitude h is the convolution of the object amplitude O with the amplitude transmission of the zone plate, $1 \pm z$. The image amplitude is the convolution of h with a reconstruction function r. For the positive zone plate this becomes-

$$h_+ = O * (1 + z)$$

$$i_+ = h_+ * r = \underbrace{O * 1 * r}_{\text{background}} + \underbrace{O * z * r}_{\text{desired image}}$$

The positive zone plate amplitude transmission is

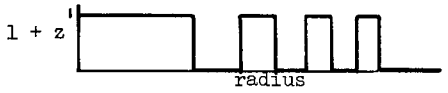

The negative zone plate amplitude transmission is

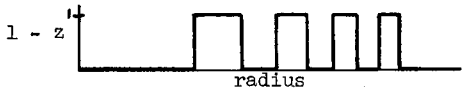

Thus, if one takes an exposure with a positive zone plate and obtains the hologram matrix $h_+ = O * (1 + z)$ and a subsequent exposure with a negative zone plate, $h_- = O * (1 - z)$, then the hologram matrix which is the difference of these two matrices yields an image which has no background.

$$h = h_+ - h_-$$

$$i = h * r = O * 2z * r$$

We have done this with holograms generated by the computer and the resulting image is given in Fig. 6. In contrast, the same object has been taken under the same conditions but using only a positive zone plate and its image is in Fig. 7. Cross-sections through these images are given in Fig. 8 and show clearly the background eliminated with this method.

Imaging with the Multi-wire Proportional Chamber

We use the multi-wire proportional chamber with delay line readout as our gamma-ray detector. It can be made inexpensively in the moderately large areas necessary and it has the fairly high resolution (1 mm) which is required. Data-taking rates of about 10^5/sec are possible. For Nuclear Medicine applications of zone plate imaging this is a limitation since objects of about 600 resolution areas take 10 min to get a reasonable signal/noise ratio ($(S/N)_B = 10$).

Fig. 9 is a photograph of our chamber and its associated electronics. The chamber is filled to 5 lbs/in^2 (gauge) with 90% Xenon and 10% CO_2 gas. The active area is 30 cm x 30 cm and is 2.5 cm thick. The efficiency for our test source, 22 KeV gammas from ^{109}Cd, is about 30% and is uniform over the face of the chamber to better than 5%. Energy resolution is about 15%. Detailed descriptions of these chambers and delay lines have been given elsewhere.[5]

The readout electronics consist of voltage sensitive pre-amplifiers, zero-crossing discriminators, pile-up rejection and coincidence circuit, dual time-to amplitude converters, and an oscilloscope display for visual recording of the hologram. Magnetic tape recording for computer reconstruction uses a 200 MHz clock, gated scalers, and interfacing electronics.

The chamber was used to record digitally 314,000 events from an array of 36 point sources using a 5 zone plate aperture. The points were spaced 2.5 resolution lengths apart. The image from the computer reconstruction is shown in Fig. 10. The signal/noise ratio is about 40% of that expected theoretically for the same statistics. The frequency-filtered image is given in Fig. 11. The faintness of the left hand row of points is probably caused by not having them within the field of view and by too strong frequency filtering.

Conclusion

Our Monte-Carlo calculation of the signal/noise ratio for zone plate imaging, using point objects distributed approximately uniformly over the field of view, for smaller numbers of object points is in fair agreement with Barrett's formula. For larger numbers of object points our results are generally smaller than the theoretical value, by about 50%, for larger numbers of events. Some discrepancy is to be expected since the formula is approximate and since the signal/noise ratio depends to some extent on the object chosen.

We have shown that the positive negative on-axis zone plate combination can be used, with detectors having digital readout, to image objects with spatial frequencies from DC to the limit imposed by the system resolution, without the large background usually associated with the on-axis zone plate. Advantages, when compared with the off-axis system, are the higher object transmissions possible, about a factor of 4, since a half-tone screen at the object is not necessary, and the higher resolutions available, about a factor of 3, with the on-axis system.

References

1. H.J. Caulfield and A.D. Williams, Optical Engineering 12, 3-7 (1973).
   H.H. Barrett, D.T. Wilson, G.H. DeMeester, and H.Sharfman, Optical Engineering 12, 8-12 (1973).
   W.L. Rogers, L.W. Jones, and W.H. Beierwaltes, Optical Engineering 12, 13-22 (1973).
2. W.L. Rogers et al. ibidem.
3. R.C. Singleton, I.E.E.E. Trans. AU-17, 93-103 (1969).
4. H.H. Barrett and F.A. Horrigan, Applied Optics, to be published.
5. A. Rindi, V. Perez-Mendez, and R. Wallace, Nucl. Inst. & Meth. 77, 325 (1970).
   R. Grove, I. Ko, B. Leskovar, and V. Perez-Mendez, Nucl. Inst. & Meth. 99, 381 (1972).

Figure Captions

Fig. 1 Making a Fresnel Zone Plate Hologram. For the detector to collect all gamma-rays passing through the zone plate the object must lie within the field of view V and the object plane must lie to the left of point A. The left-most position B of the object plane is determined by the requirement that the detector must be able to resolve the finest zone of the zone plate.

Fig. 2 Optical Analogue of Image Reconstruction by Computer. Light diffracted by the zone plate shadow A of a point source emerges in a parallel beam and is focussed to a point at P by the Fourier transform lens.

Fig. 3 Image of a 256 Point Square Array. The computer was used to generate hologram events using a 10-ring zone plate (N_z = 19) and a detector matrix size 256 x 256. The choice of the parameter S = 0.60 gave a field of view having about 45 x 45 resolution areas. The spacing of the object points was chosen so as to cover the field of view. 16.2 million events were used to produce this image which has a measured signal/noise ratio of 5.9 ± 0.4 .

Fig. 4 Frequency Filtered Image. The low spatial frequency components of Fig. 3 have been reduced by frequency filtering (through the first harmonic). A much greater reduction of background could have been made if higher harmonics had been eliminated.

Fig. 5 Cross-Section Plots of Images. Top graph is a plot of Fig. 3 and shows the effect of noise and the image superimposed on a large background. Bottom graph is a plot of the frequency filtered image.

Fig. 6 Background Elimination Using an On-Axis Positive-Negative Zone Plate Combination. 300,000 events were generated by computer using 3-ring positive and negative zone plates. Resolution is 3.2 raster units. The image with its low spatial frequencies is obtained free of background without frequency filtering.

Fig. 7 Image from On-Axis Positive Zone Plate. In comparison with Fig. 6 which has the same object and the same imaging system, the image is seen to be superimposed on a large background.

Fig. 8 Cross-Sections of Images. The top plot, a cross-section of Fig. 6, has used the positive-negative zone plate combination. The bottom plot, a cross-section of Fig. 7, shows clearly the large background associated with the same object when only a positive zone plate is used.

Fig. 9 Multiwire Proportional Chamber and Associated Electronics. The chamber, zone plate, and radioactive object are in the wooden frame on the left. The two electronics racks on the right will independently record the hologram on magnetic tape or oscilloscope display.

Fig. 10 Image of a 6 x 6 Array Recorded with the Multiwire Proportional Chamber.

Fig. 11 Frequency Filtered Image of the 6 x 6 Array.

TABLE I

Object field-of-view parameter, $S = (V/D)/(1 + S_1/S_2)$; the maximum number of object resolution lengths, N_{max}, and Fresnel zones, N_z, resolvable with a detector having N_d resolution lengths.

	$N_d = 32$		$N_d = 64$		$N_d = 128$		$N_d = 256$	
S_{max}	N_{max}	N_z	N_{max}	N_z	N_{max}	N_z	N_{max}	N_z
0	0.	8.0	0.	16.0	0.	32.0	0.	64.0
.016	0.5	7.9	1.	15.8	2.	31.5	4.	63.0
.032	1.0	7.8	2.	15.5	4.	31.0	8.	62.0
.049	1.5	7.6	3.	15.3	6.	30.5	12.	61.0
.067	2.0	7.5	4.	15.0	8.	30.0	16.	60.0
.103	3.	7.3	6.	14.5	12.	29.0	24.	58.0
.143	4.	7.0	8.	14.0	16.	28.0	32.	56.0
.23	6.	6.5	12.	13.0	24.	26.0	48.	52.0
.33	8.	6.0	16.	12.0	32.	24.0	64.	48.0
.60	12.	5.0	24.	10.0	48.	20.0	96.	40.0
1.00	16.	4.0	32.	8.0	64.	16.0	128.	32.0

Table II

Theoretical signal/noise ratio $(S/N)_B$; the measured signal/noise ratio in units of $(S/N)_B$ for various numbers of object points M. Events generated by computer using the indicated imaging systems.

	S = 0.60 N_z = 5 N_d = 64				S = 0.60 N_z = 19 N_d = 256			
	M				M			
$(S/N)_B$	9	16	25	36	64	100	169	256
2.0	1.04 ±.10	1.19 ±.12	1.26 ±.13	1.46 ±.15	0.99 ±.09	1.17 ±.12	0.74 ±.06	1.21 ±.08
4.0	1.28 ±.13	1.24 ±.12	1.34 ±.13	1.42 ±.14	0.88 ±.08	0.93 ±.09	0.67 ±.05	1.02 ±.06
6.0	1.26 ±.13	1.24 ±.12	1.12 ±.11	1.17 ±.12	0.76 ±.07	0.80 ±.08	0.54 ±.04	0.91 ±.06
8.0	0.91 ±.09	1.23 ±.12	1.22 ±.12	1.04 ±.10	0.65 ±.06	0.76 ±.08	0.43 ±.03	0.75 ±.05
10.0	0.80 ±.08	1.15 ±.12	1.17 ±.12	0.98 ±.10	0.55 ±.05	0.70 ±.07	0.37 ±.03	0.66 ±.04

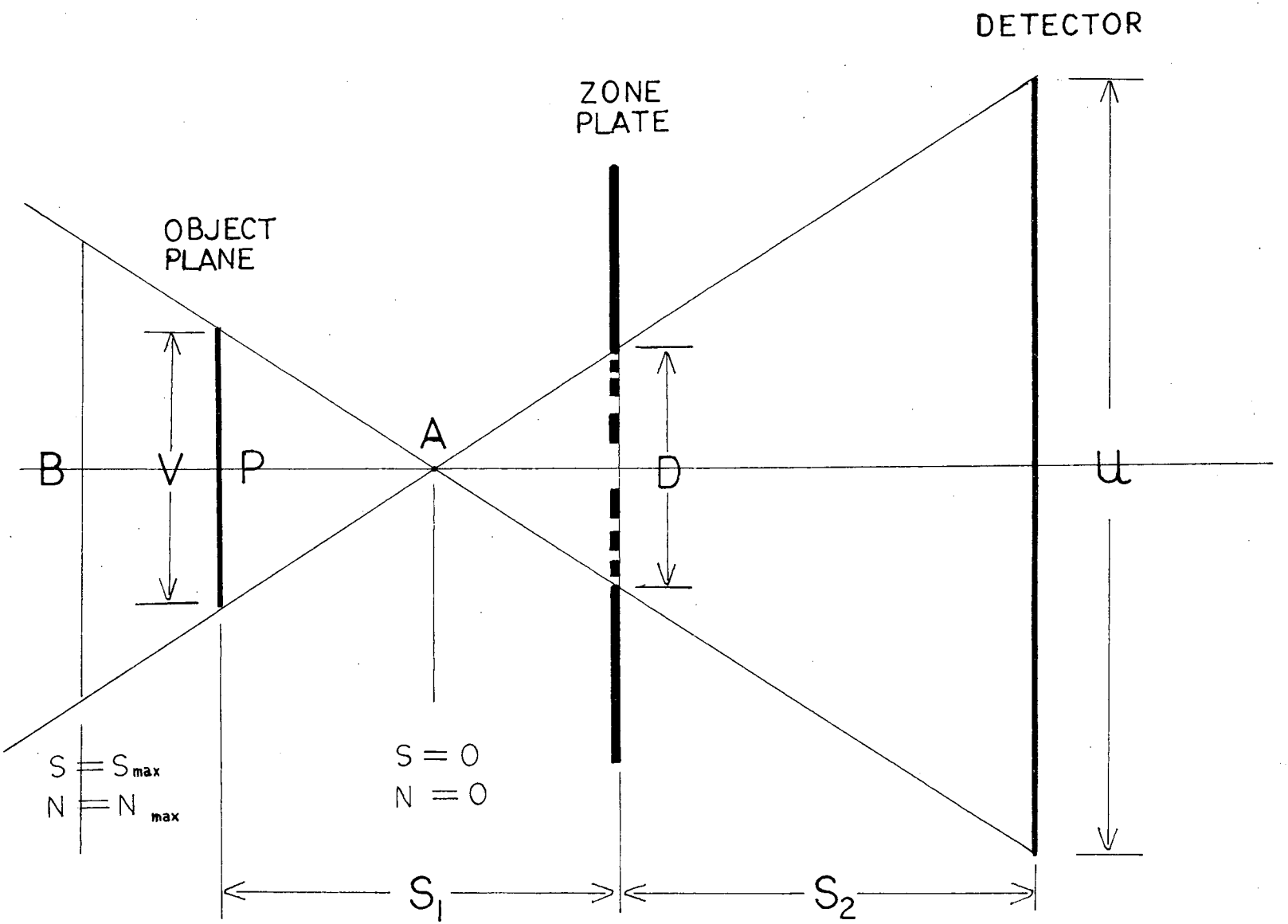
DETECTOR
ZONE
PLATE
OBJECT
PLANE
B
V
P
A
D
u
S = S max
N = N max
S = 0
N = 0
S1
S2
XBL 7311-1445

FIG. 1

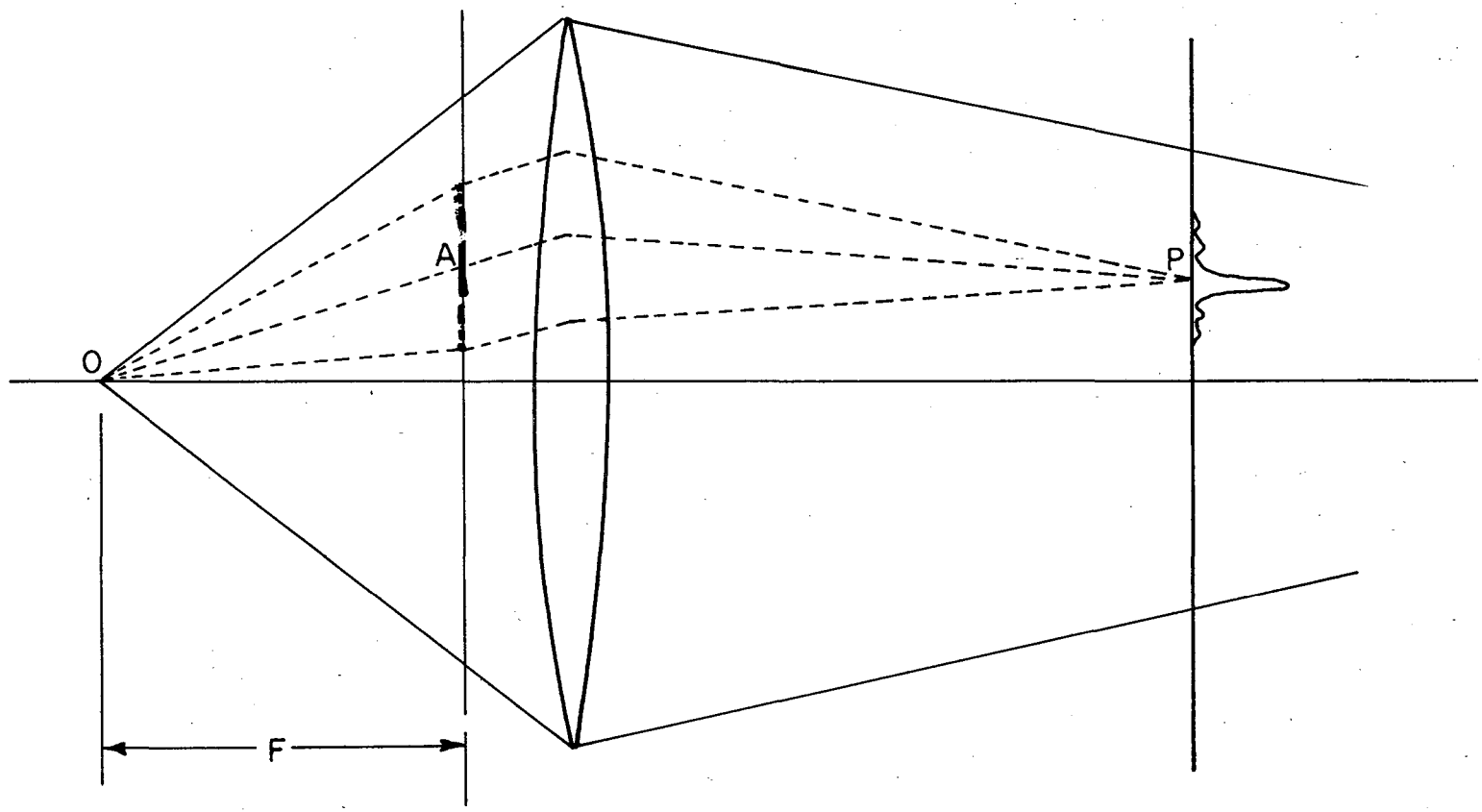

XBL 7311-6802

FIG. 2

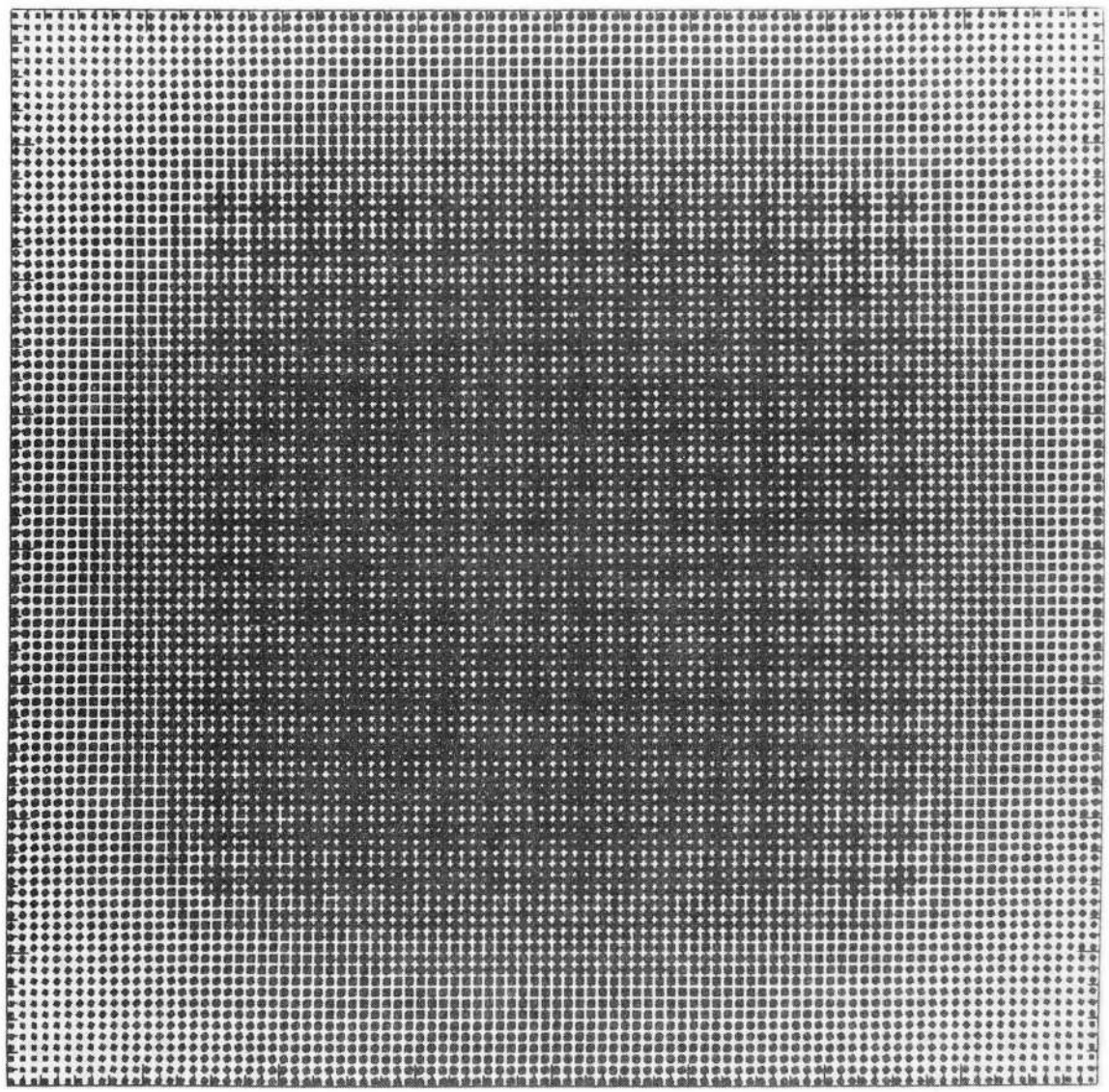

FIG. 3

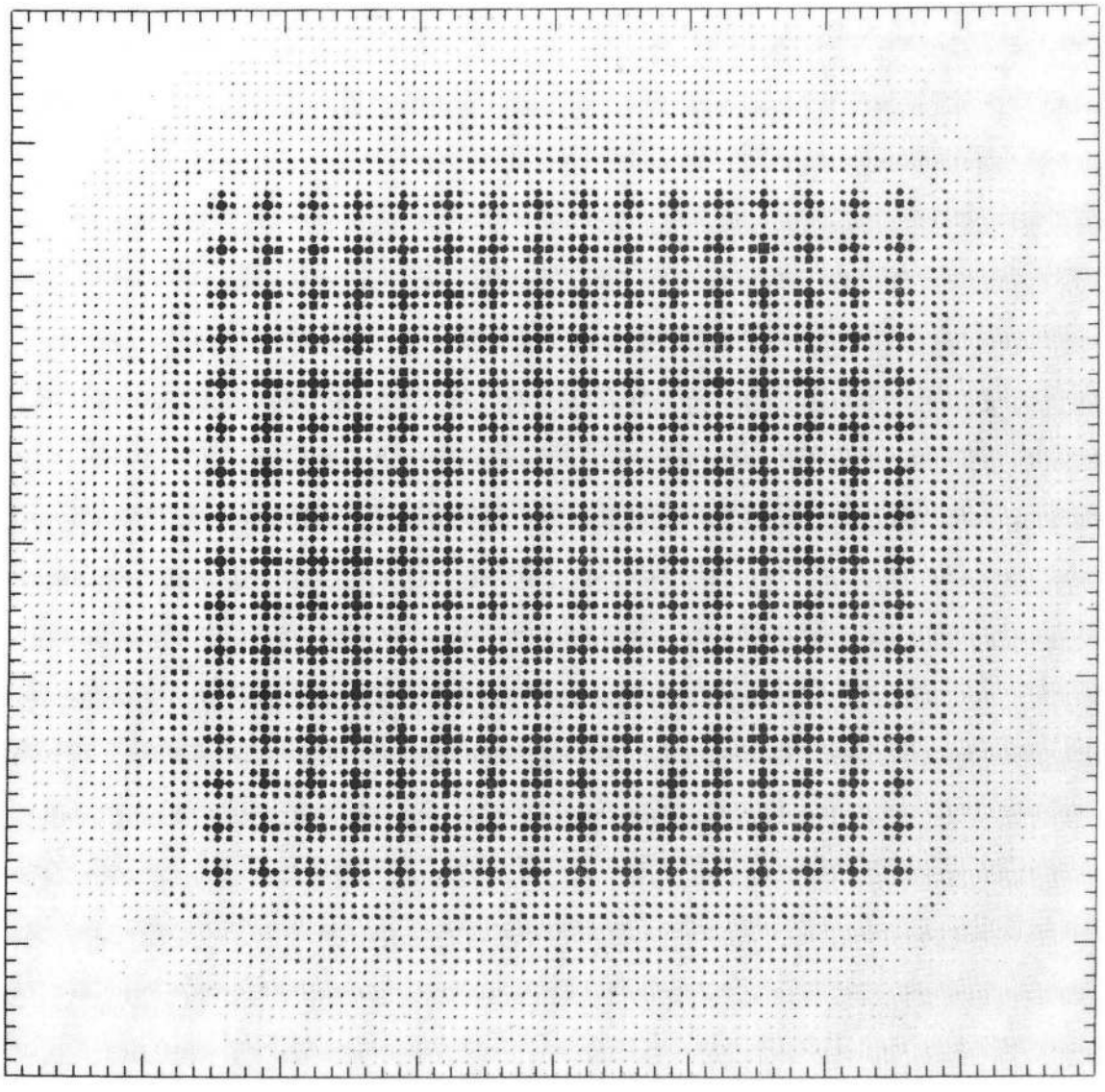

FIG. 4

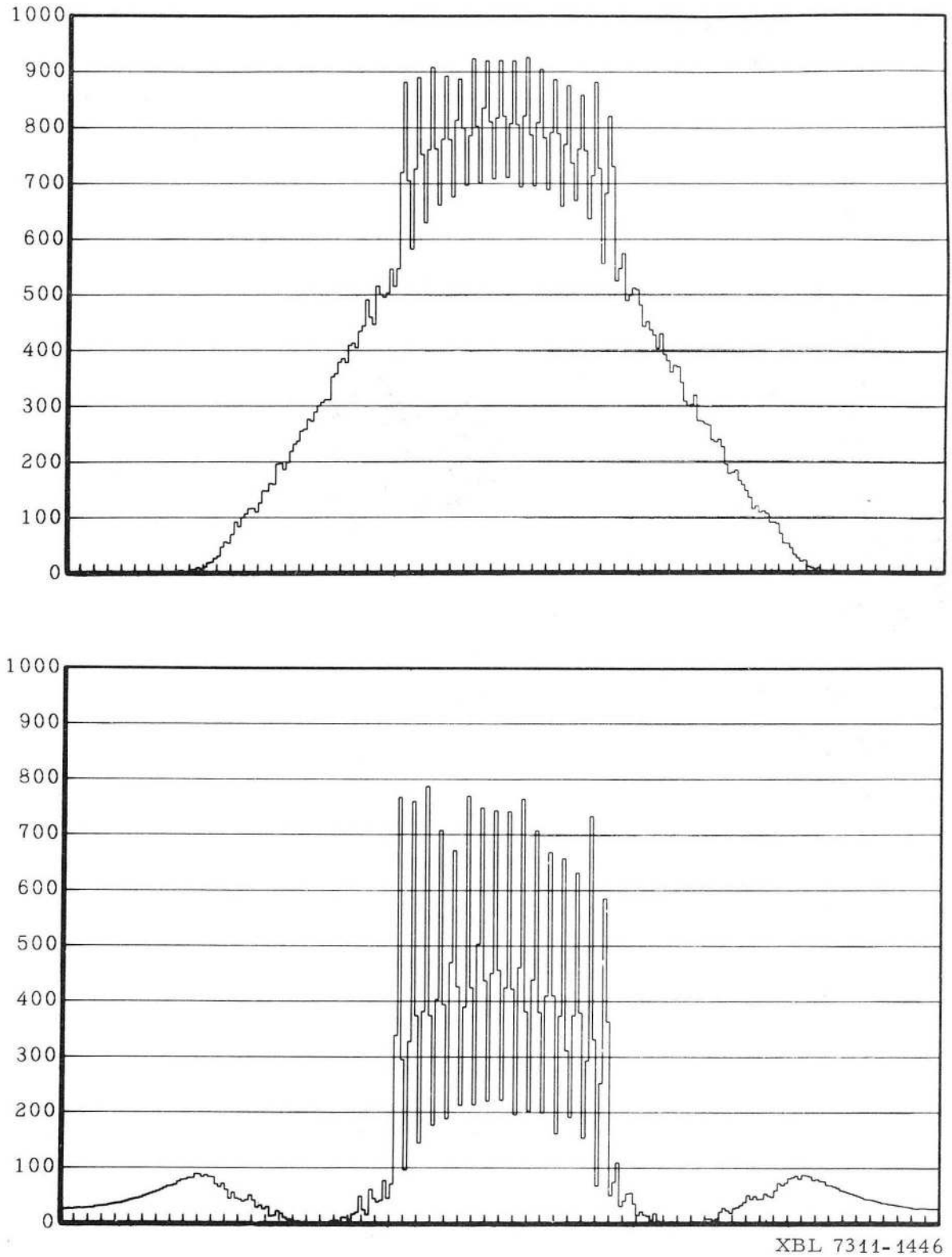
1000
900
800
700
600
500
400
300
200
100
0
1000
900
800
700
600
500
400
300
200
100
0
XBL 7311-1446

FIG. 5

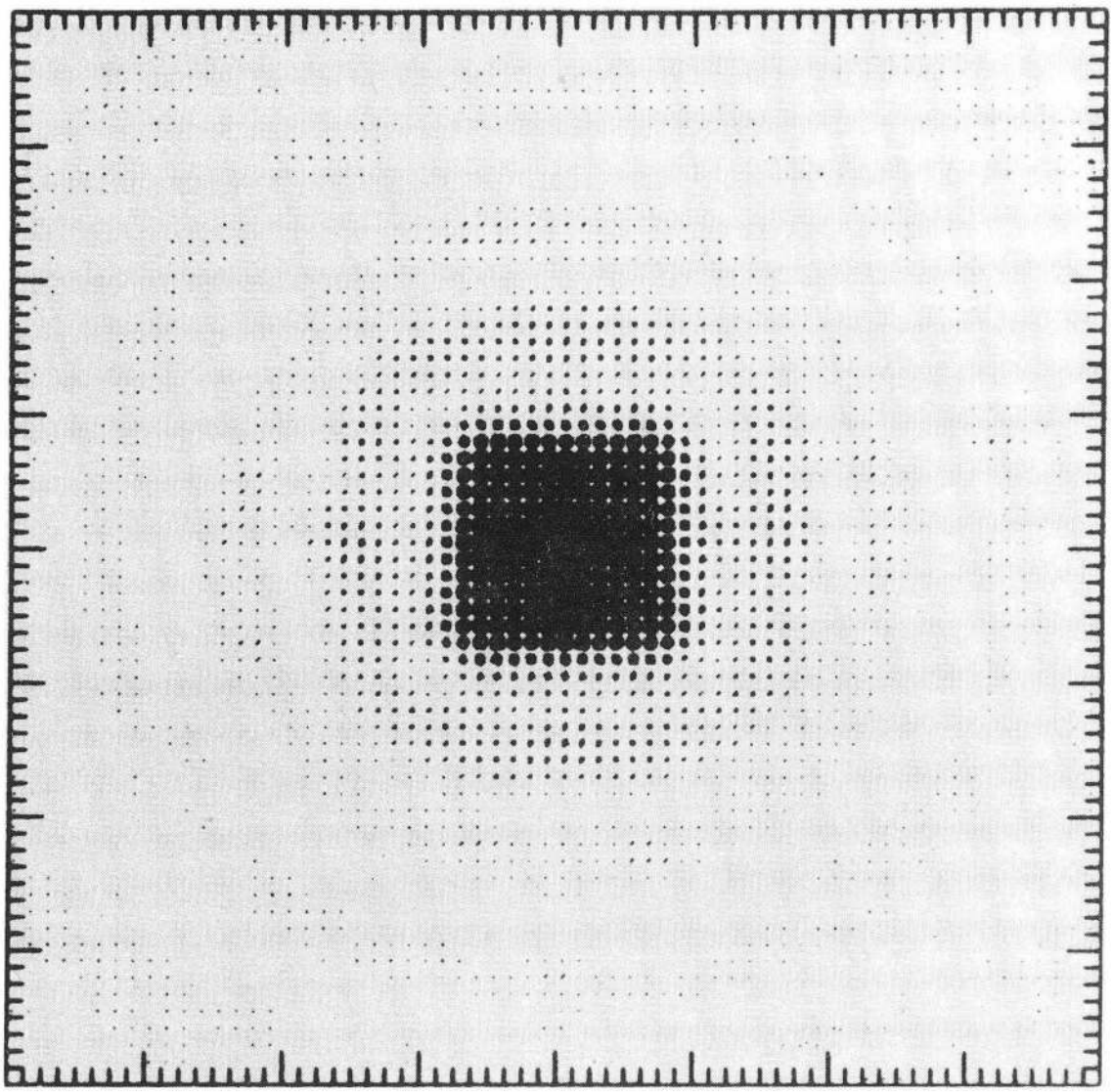

FIG. 6

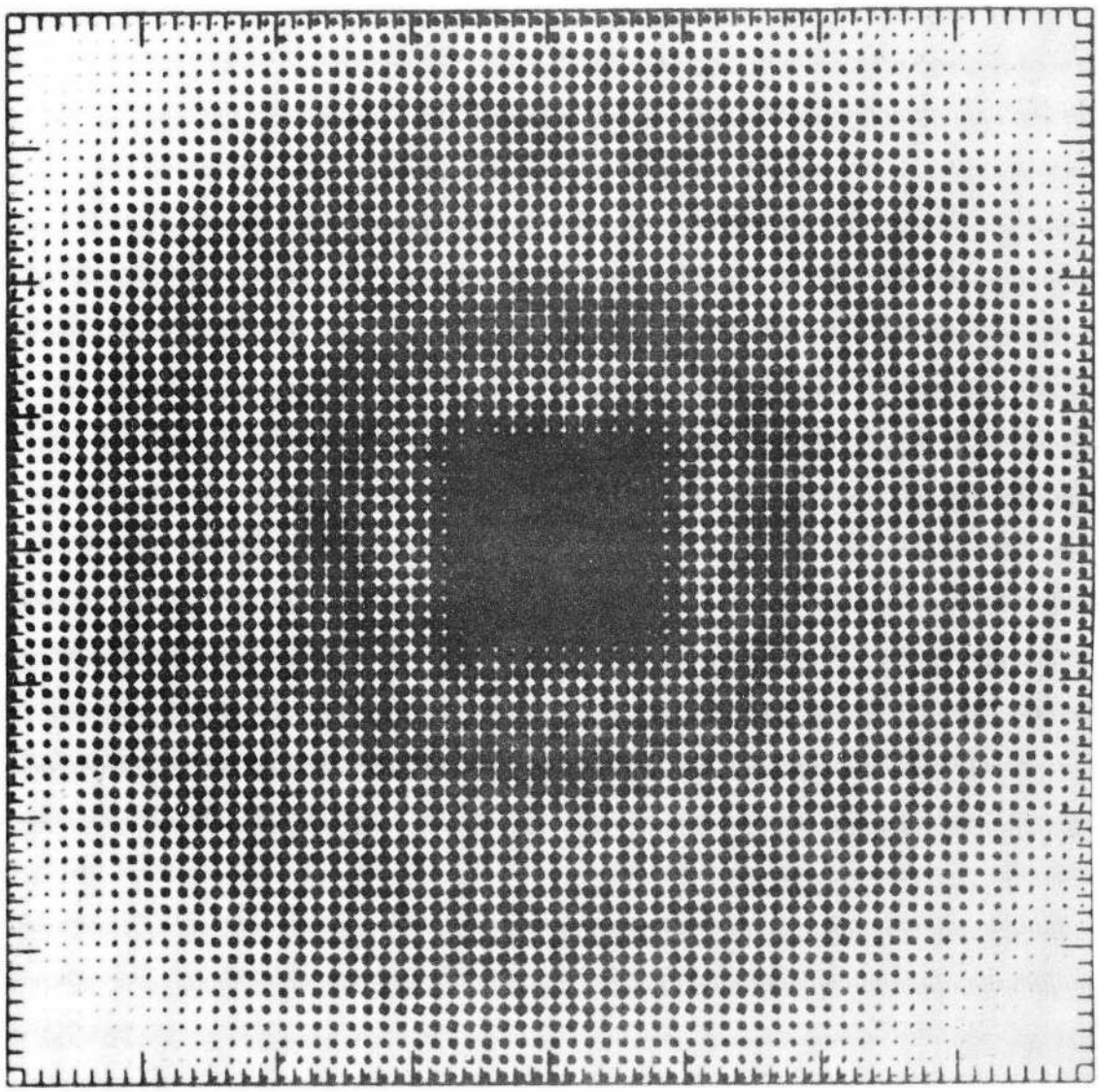

FIG. 7

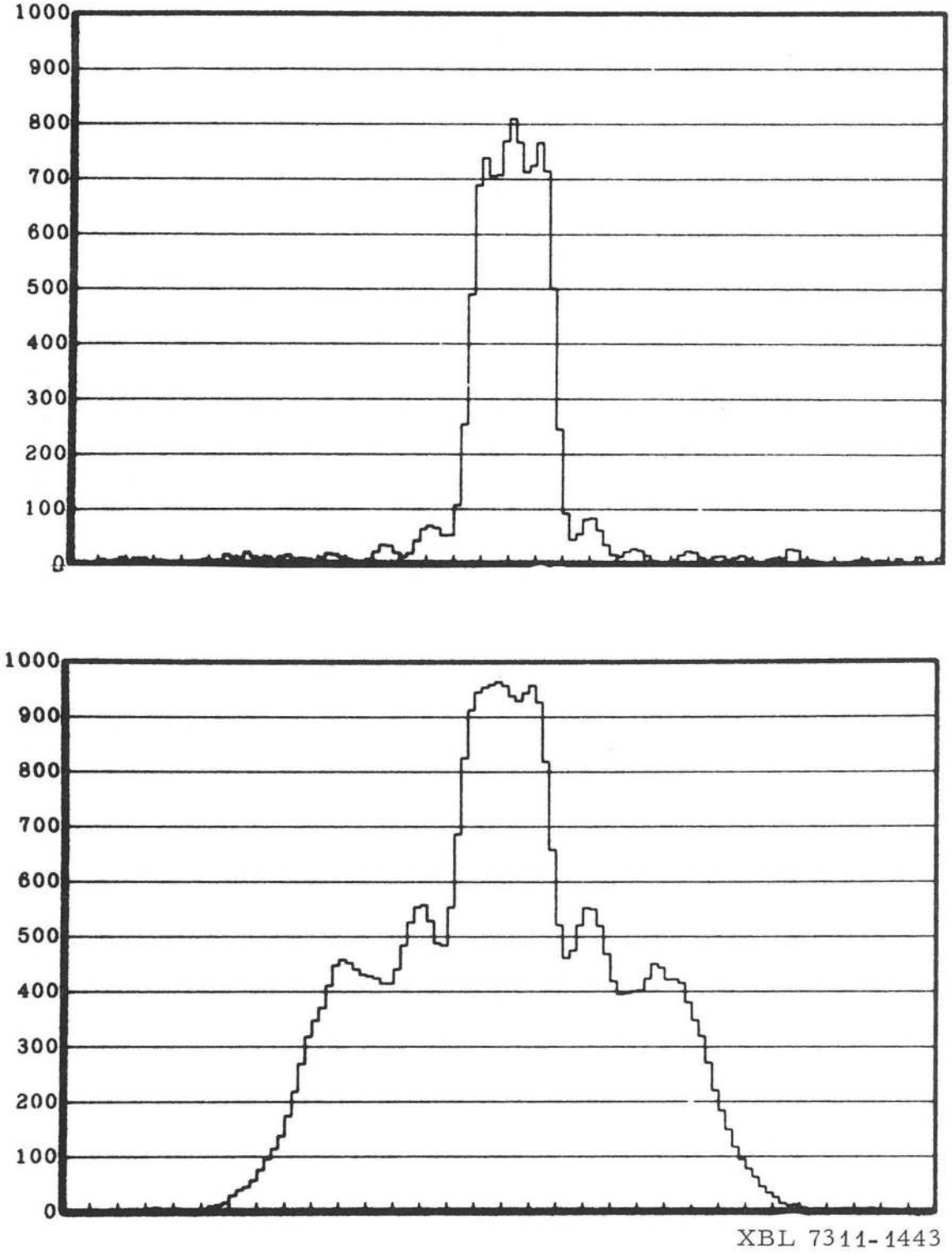
1000
900
800
700
600
500
400
300
200
100
0
1000
900
800
700
600
500
400
300
200
100
0
XBL 7311-1443

FIG. 8

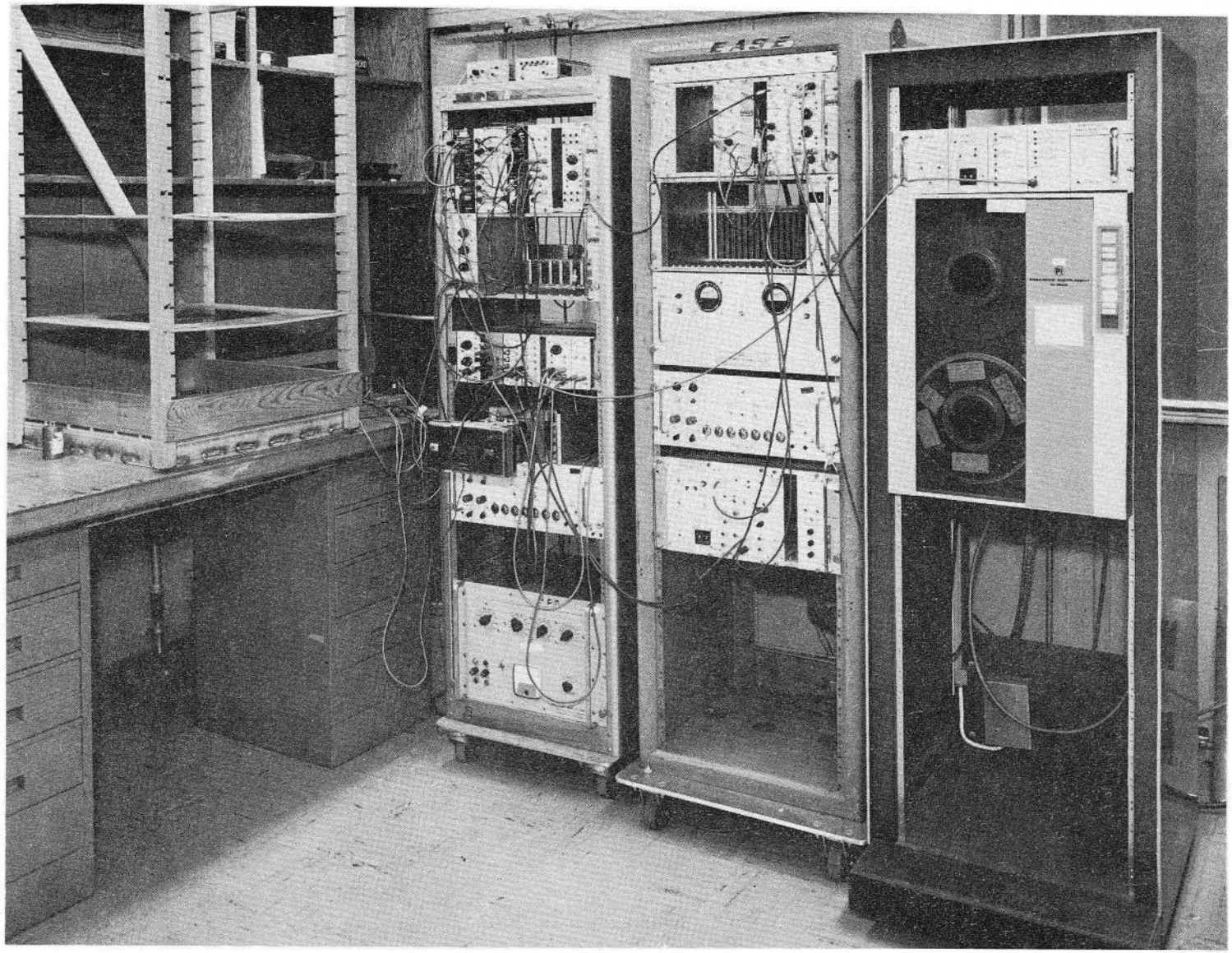

FIG. 9

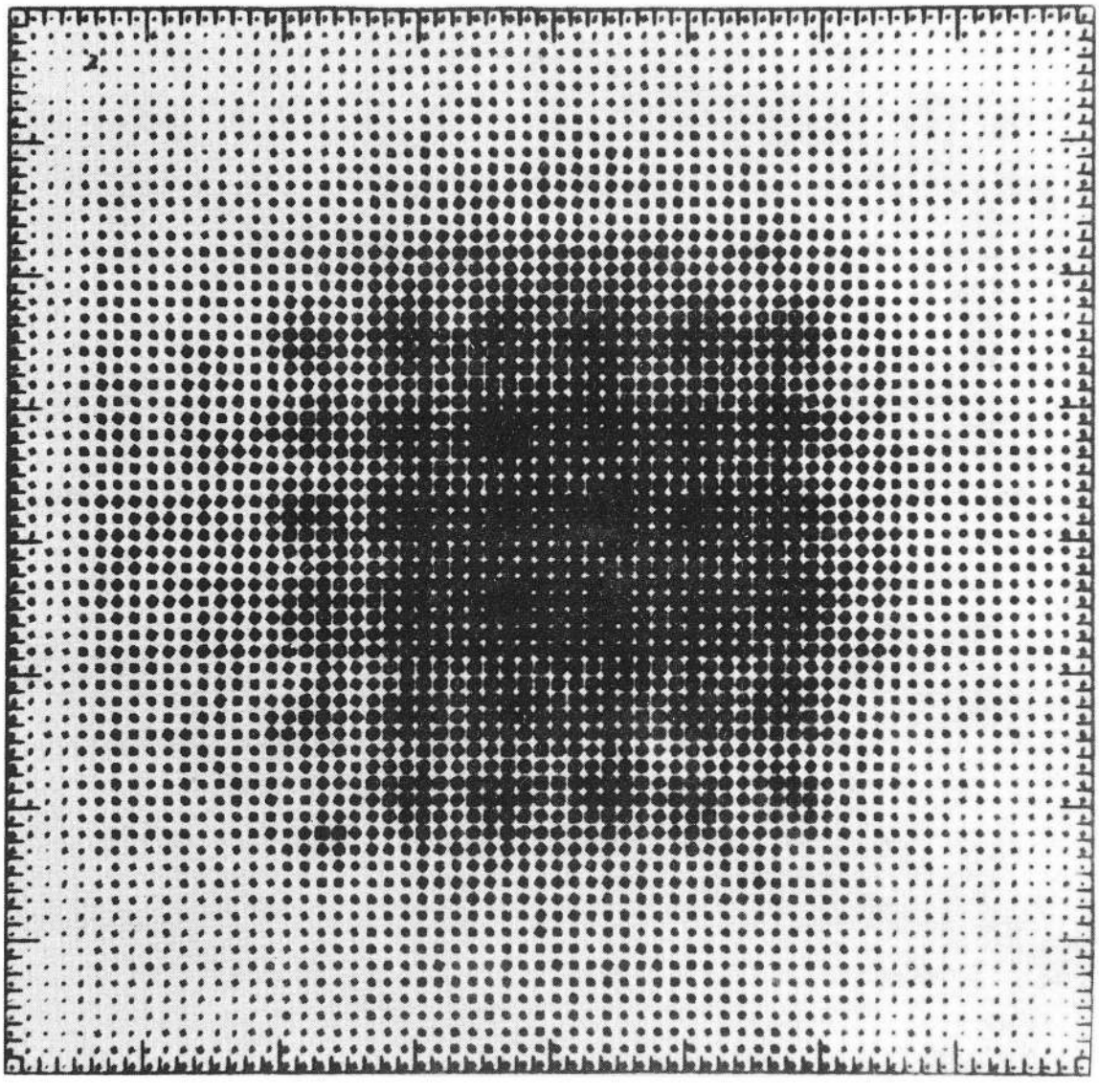

FIG. 10

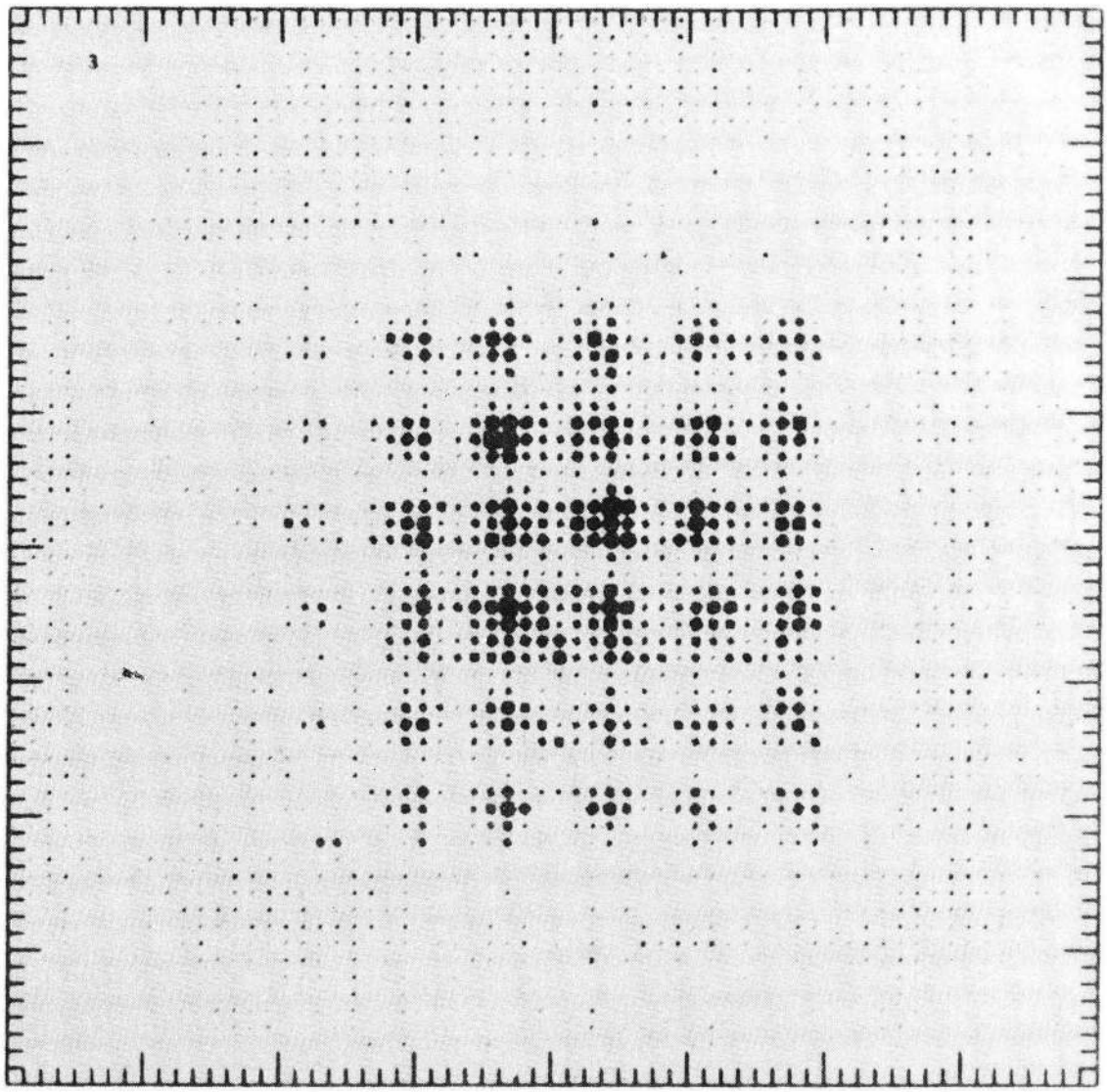

FIG. 11

TECHNICAL INFORMATION DIVISION
LAWRENCE BERKELEY LABORATORY
UNIVERSITY OF CALIFORNIA
BERKELEY, CALIFORNIA 94720